Simulation of GPS signal in a forest environment using a coherent fractal tree model

Arnaud Coatanhay
E3I2 - ENSIETA
29806 Brest Cedex 9, France
Email: arnaud.coatanhay@ensieta.fr
Telephone: (33) 2 98 34 87 20 Fax: (33) 2 98 34 87 59

***Abstract*— This paper presents an electromagnetic model for the GPS signal propagation in forest environment. This model is based on a fractal description of tree structure seen as a cluster of scatterers composed by cylinders (trunk and branches). The model of the scattering by these finite length cylinders is based on the infinite cylinder approximation. More, soil is considered as a plane dielectric interface. Finally, we estimate the GPS signal received in the vicinity of tree bottoms.**

I. Introduction

In forest environments, GPS devices has become a very common use equipment for many different activities: monitoring forestry harvesting, forest rambling,... However due to attenuation and multipath problems, a forest environment raises great problems for GPS receivers that often lead to positioning mistakes or inoperability. To design more robust GPS receivers, a reliable forest GPS signal simulators is of the most importance.

This paper presents a GPS simulation that takes into account the coherent scattering by the trees and the soil interface. To generate a realistic GPS signal, temporal code sequence and ionospheric scintillation phenomenon problems are considered.

II. Fractal tree model

For GPS (L-band), the scattering in forest environment is mainly due to trunks and branches. In our study, scattering by leaves is neglected. So, a forest is composed by different trees and each tree is considered as a cluster of cylinders (trunk and branches).

An appropriate approach to simulate actual trees is the random fractal model [1]. The generation of a tree model is initially determined by the trunk, considered as a dielectric cylinder (radius and height are respectively denoted r_0 and l_0). Then, trunk is split into n branches (dielectric cylinders) whose heights, denoted l_{1i} ($i = 1, 2, \ldots, n$), are given by the following equation:

$$l_{1i} = k_{lm} \cdot (1 + \varepsilon_{li} \cdot RND) \cdot l_0 \quad (1)$$

where RND is a random value between 0 and 1, ε_{li} is the random amplitude and k_{lm} is the mean ratio between the trunk and branch heights. The radius of the branches r_{1i} are determined in the same way using:

$$r_{1i} = k_{rm} \cdot (1 + \varepsilon_{ri} \cdot RND) \cdot r_0 \quad (2)$$

where k_{rm} is the mean ratio between the trunk and branch radius. More, each branch is of an angle α_{1i} from the trunk axis:

$$\alpha_{1i} = \alpha_m \cdot \frac{\pi}{2} \left(1 + \varepsilon_{\alpha i} \cdot RND\right) \quad (3)$$

where α_m is the mean value of the angle.

The equations (1), (2) and (3) lead to an iterative process as described in the figure (1).

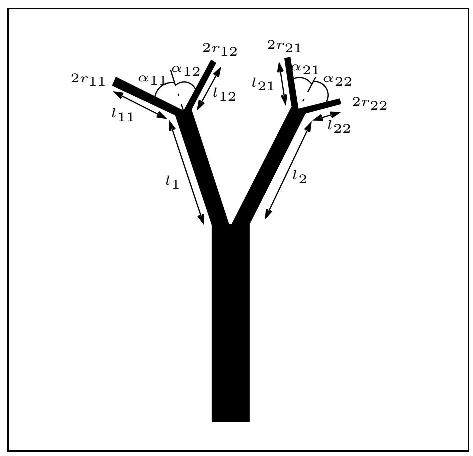

Fig. 1. *Fractal tree generated by the iterative process at the second step with 2 branches at each step.*

In that way, random fractal trees can be generated from several, previously given, parameters (contraction ratio for branches, branching angle from the trunk, etc...).

III. Electromagnetic scattering

The scattering by a forest boils down to the sum of the scattering by finite length cylinders.

A. Scattering by a cylinder

To estimate the scattering matrix of each finite length cylinder $\mathbf{f}\left(\theta_s, \phi_s, \pi - \theta_i, \phi_i\right)$ (θ_i, ϕ_i incident direction and θ_s, ϕ_s scattered direction), we use the infinite cylinder approximation [2].

1) Infinite cylinder: Letting an incident plane wave $\vec{E}_i$

$$\vec{E}_i = \left(E_{vi}\vec{v}_i + E_{hi}\vec{h}_i\right) \cdot e^{i\vec{k}_i \cdot \vec{r}} \tag{4}$$

where $\vec{v}_i$ and $\vec{h}_i$ are unit polarisation vectors.

In modal theory, the electromagnetic field $\vec{E}_s$ scattered by an infinitely long dielectric cylinder can be expressed as a modal series:

$$\begin{aligned}\vec{E}_s = \sum_{n=-\infty}^{+\infty} \frac{i^n e^{-in\phi_i}}{k_{i\rho}} \Big[& a_n^{(M)} \vec{M}_n \left(k_{i\rho}, k_{iz}, \vec{r}\right) \\ & + a_n^{(N)} \vec{N}_n \left(k_{i\rho}, k_{iz}, \vec{r}\right)\Big]\end{aligned} \tag{5}$$

In the same way, the interior electromagnetic field $\vec{E}_{int}$ is in the form:

$$\begin{aligned}\vec{E}_{int} = \sum_{n=-\infty}^{+\infty} \frac{i^n e^{-in\phi_i}}{k_{i\rho}} \Big[& c_n^{(M)} Rg\vec{M}_n \left(k_{ip\rho}, k_{iz}, \vec{r}\right) \\ & + c_n^{(N)} Rg\vec{N}_n \left(k_{ip\rho}, k_{iz}, \vec{r}\right)\Big]\end{aligned} \tag{6}$$

where $k_{ip\rho} = \sqrt{k_{ip}^2 - k_{iz}^2}$ and $k_{ip} = \sqrt{\epsilon_p/\epsilon_0} \cdot k$. $Rg\vec{M}_n$, $\vec{M}_n$, $Rg\vec{N}_n$, $\vec{N}_n$ are the regular (denoted Rg) or non regular vector cylindrical wave functions. $c_n^{(M)}$ and $c_n^{(N)}$ coefficients are solutions the following linear system:

$$\begin{aligned}\frac{E_{hi}}{k_{i\rho}} i^{n+1} e^{-in\phi_i} = & A_n^{MM}\left(k_{i\rho}, k_{iz}, k_{ip\rho}, k_{iz}, a\right) c_n^{(M)} \\ & + A_n^{MN}\left(k_{i\rho}, k_{iz}, k_{ip\rho}, k_{iz}, a\right) c_n^{(N)}\end{aligned} \tag{7a}$$

$$\begin{aligned}\frac{E_{vi}}{k_{i\rho}} i^{n} e^{-in\phi_i} = & A_n^{NM}\left(k_{i\rho}, k_{iz}, k_{ip\rho}, k_{iz}, a\right) c_n^{(M)} \\ & + A_n^{NN}\left(k_{i\rho}, k_{iz}, k_{ip\rho}, k_{iz}, a\right) c_n^{(N)}\end{aligned} \tag{7b}$$

where A_n^{MM}, A_n^{MN},A_n^{NM} and A_n^{NN} are given by:

$$\begin{aligned}A_n^{MM} & \left(k_{0\rho}, k_{iz}, k'_{p\rho}, k'_z, a\right) = \\ & -\frac{ia\pi}{2k_{0\rho}^2}\Big[k'^2_{p\rho} k_{0\rho} J_n\left(k'_{p\rho}a\right) H_n^{(1)\prime}\left(k_{0\rho}a\right) \\ & -k'_{p\rho} k_{0\rho}^2 J'_n\left(k'_{p\rho}a\right) H_n^{(1)}\left(k_{0\rho}a\right)\Big]\end{aligned} \tag{8a}$$

$$\begin{aligned}A_n^{MN} & \left(k_{0\rho}, k_{iz}, k'_{p\rho}, k'_z, a\right) = \\ & -\frac{ia\pi}{2k_{0\rho}^2}\left[\frac{n}{k_p a}\left(k'^2_{p\rho} k_z - k'_z k_{0\rho}^2\right)\right. \\ & \left. J_n\left(k'_{p\rho}a\right) H_n^{(1)}\left(k_{0\rho}a\right)\right]\end{aligned} \tag{8b}$$

$$\begin{aligned}A_n^{NN} & \left(k_{0\rho}, k_{iz}, k'_{p\rho}, k'_z, a\right) = \\ & \frac{k_p}{k} A_n^{MN}\left(k_{0\rho}, k_{iz}, k'_{p\rho}, k'_z, a\right)\end{aligned} \tag{8c}$$

$$\begin{aligned}A_n^{NN} & \left(k_{0\rho}, k_{iz}, k'_{p\rho}, k'_z, a\right) = \\ & -\frac{ia\pi}{2k_{0\rho}^2}\left[\frac{kk_{0\rho}}{k_p} k'^2_{p\rho} J_n\left(k'_{p\rho}a\right) H_n^{(1)\prime}\left(k_{0\rho}a\right)\right. \\ & \left. -\frac{k_p k'_{p\rho}}{k} k_{0\rho}^2 J'_n\left(k'_{p\rho}a\right) H_n^{(1)}\left(k_{0\rho}a\right)\right]\end{aligned} \tag{8d}$$

2) Finite dielectric cylinder: Assuming the interior electromagnetic field is estimated, the far-field scattered field can be obtained by integrating over the finite surface of the cylinder excluding the end caps. Finally, this integration leads to:

$$\begin{aligned}\vec{E}_s = & \frac{e^{ikr}}{4\pi r}\frac{ikL}{\pi}\sin\theta_s \operatorname{sinc}\left[\left(k_{iz} - k_{sz}\right)\frac{L}{2}\right] \sum_{n=-\infty}^{+\infty} (-i)^n e^{in\phi_s} \\ & \Big\{-i\vec{h}_s\Big[RgA_n^{MM}\left(k_{s\rho}, k_{sz}, k_{ip\rho}, k_{iz}, a\right) c_n^{(M)} \\ & +RgA_n^{MN}\left(k_{s\rho}, k_{sz}, k_{ip\rho}, k_{iz}, a\right) c_n^{(N)}\Big] \\ & -\vec{v}_s\Big[RgA_n^{NM}\left(k_{s\rho}, k_{sz}, k_{ip\rho}, k_{iz}, a\right) c_n^{(M)} \\ & +RgA_n^{NN}\left(k_{s\rho}, k_{sz}, k_{ip\rho}, k_{iz}, a\right) c_n^{(N)}\Big]\Big\}\end{aligned} \tag{9}$$

where RgA_n^{MM}, RgA_n^{MN},RgA_n^{NM} et RgA_n^{NN} are the expression in (8a,8c,8b,8d), respectively, with $H_n^{(1)}$ replaced by J_n.

So, using equation (9), the scattered field be expressed as:

$$\begin{aligned}\begin{bmatrix}E_{vs}\\E_{hs}\end{bmatrix} & \simeq \frac{e^{ikR}}{R}\begin{bmatrix}f_{vv} & f_{vh}\\ f_{hv} & f_{hh}\end{bmatrix}\cdot\begin{bmatrix}E_{vi}\\E_{hi}\end{bmatrix} \\ & = \mathbf{f}\left(\theta_s, \phi_s, \pi - \theta_i, \phi_i\right)\cdot\begin{bmatrix}E_{vi}\\E_{hi}\end{bmatrix}\end{aligned} \tag{10}$$

B. Soil influence

Interaction between cylinder is neglected, but we take into account reflexions by the ground (dielectric plane interface). So the total scattering by a cylinder $\mathbf{F}\left(\theta_s, \phi_s, \pi - \theta_i, \phi_i\right)$ is in the form:

$$\begin{aligned}\mathbf{F}\left(\theta_s, \phi_s, \pi - \theta_i, \phi_i\right) = & \mathbf{f}\left(\theta_s, \phi_s, \pi - \theta_i, \phi_i\right)\cdot e^{i\tau_1} \\ & + \mathbf{f}\left(\theta_s, \phi_s, \theta_i, \phi_i\right)\cdot\mathbf{R}\left(\theta_i\right)\cdot e^{i\tau_2} \\ & + \mathbf{R}\left(\theta_s\right)\cdot\mathbf{f}\left(\pi - \theta_s, \phi_s, \pi - \theta_i, \phi_i\right)\cdot e^{i\tau_3} \\ & + \mathbf{R}\left(\theta_s\right)\cdot\mathbf{f}\left(\pi - \theta_s, \phi_s, \theta_i, \phi_i\right)\cdot\mathbf{R}\left(\theta_i\right)\cdot e^{i\tau_4}\end{aligned} \tag{11}$$

where $\mathbf{R}$ is the Fresnel coefficient matrix, and $(\tau_1, \tau_2, \tau_3, \tau_4)$ are phases related to the different ray paths, see figure (2).

Finally, global vegetation (leaves, thin branches...) is modeled by a continuous random medium and the Foldy's approximation [3]. More precisely, this model involves a continuous attenuation function that depends on the altitude. In the present case, this function is represented in the figure (3).

C. Summation

To estimate the total contribution of a forest $\mathbf{F}_{tot}$, we considered the sum of each cylinder contribution independently.

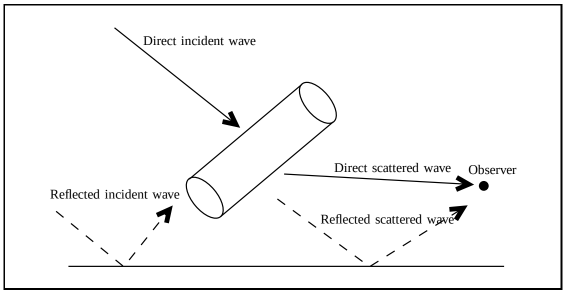

Fig. 2. *Direct and reflected fields for each cylinder.*

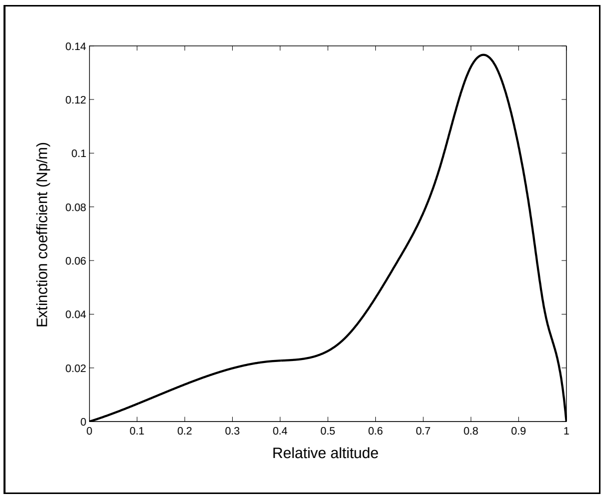

Fig. 3. *The continuous attenuation function.*

If the forest is composed by N_T trees and each tree has N_B branches, the total contribution of a forest $\mathbf{F}_{tot}$ is in the form:

$$\mathbf{F}_{tot} = \sum_{p=1}^{N_T} \sum_{q=1}^{N_B} \mathbf{F}_{pq} e^{i\vec{k}\cdot\vec{r}_{pq}} \qquad (12)$$

where the q^{th} cylinder of the p^{th} tree is situated at $\vec{r}_{pq}$ and involves a scattered field estimated with the $\mathbf{F}_{pq}$ operator.

More, the direct signal and the reflection of the direct signal must added to the forest contribution.

IV. GPS SIGNAL

Now, we can compute the propagation perturbation caused by the forest for a monochromatic electromagnetic plane wave. But, to simulate this effect for a GPS signal, we need to determine the temporal response the forest.

A. Temporal domain

In few words, the GPS signal is a monochromatic electromagnetic plane wave with a $L_1 = 1.575\,GHz$ frequency (C/A-code) that is modulated by a random sequence. To simulate GPS signal in forest, we need a high precision temporal convolution propagation model.

For this convolution model, the temporal response can be obtained using an inverse Fourier transform process, if the forest contribution is computed for a very wide frequency band around $L_1 = 1.575\,GHz$. However, the physical scattering model is not valid for this wide frequency band. So, when we compute the frequentiel response for this wide band, we assume the scattering operators $\mathbf{f}\,(\theta_s, \phi_s, \pi - \theta_i, \phi_i)$ (cylindrical scattering) are evaluted for the frequency $L_1 = 1.575\,GHz$.

In the figure (4), an example of the temporal response for the GPS signal is presented. The first peak ($t = 0$) corresponds to the direct signal for the observer. The second peak corresponds the reflection of the direct signal. The following peaks are caused by 2 trees situated near the observer.

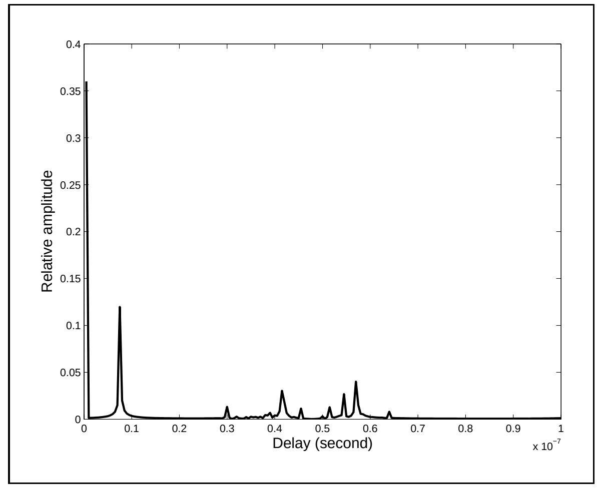

Fig. 4. *Temporal response from a medium with trees.*

A numerical GPS signal is convoluted with this temporal response to obtain the complete GPS signal in forest.

B. Atmospheric effets

To be more realistic, the ionospheric scintillation model is considered and given by the Nakagami probabilistic distribution:

$$f\,(\delta I) = \frac{m^m \delta I^{m-1}}{\Gamma\,(m)} e^{-m\delta I^2} \qquad (13)$$

where I is the relative amplitude variation and m is the fading model order.

V. CONCLUSION

The here presented electromagnetic propagation model in forest environment constitutes a realistic GPS simulator relevant with actual data.

REFERENCES

[1] P. Prusinkiewicz and A. Lindenmayer, *The Algorithmic Beauty of Plants*. New York: Springer-Verlag, 1990.

[2] L. Yi-Cheng and K. Sarabandi, “Electromagnetic scattering model for a tree trunk above a tilted ground plane,” *IEEE Trans. Geosc. Remot. Sens.*, vol. 33, no. 4, pp. 1063–1070, 1995.

[3] ——, “A monte carlo coherent scattering model for forest canopies using fractal-generated trees,” *IEEE Trans. Geosc. Remot. Sens.*, vol. 37, no. 1, pp. 440–451, 1999.